Letter to the Editor

A thermodynamic model for the O_2^- mobility in Ne gas in broad density and temperature ranges

A. F. Borghesani

CNISM Unit, Department of Physics and Astronomy
University of Padua, Italy

E-mail: armandofrancesco.borghesani@unipd.it

F.Aitken

University Grenoble Alpes, C.N.R.S., G2ELab, Grenoble, France

Abstract. We report new measurements of the mobility μ of O_2^- ions in supercritical neon in the range $45\,\mathrm{K} \leq T \leq 334\,\mathrm{K}$ for number density $N \geq 0.5\,\mathrm{nm}^{-3}$. We rationalize the experimental data of all isotherms with the Stokes-Cunningham formula by computing the ion hydrodynamic radius as a function of T and N with the thermodynamic free volume model developed for the ion mobility in superfluid He. The model parameters are determined by re-analyzing published data for $T = 45\,\mathrm{K}$ for N up to $N \approx 1.65 N_c$ ($N_c \approx 14.4\,\mathrm{nm}^{-3}$ is the critical number density), which roughly span four orders of magnitude of the Knudsen number ($0.1 \leq \mathrm{K}_n \leq 1000$), covering the transition from the kinetic- to the hydrodynamic transport regime. These parameters provide an excellent description of the dependence of μ on N for all higher isotherms and yield a strict test of the model validity, thereby bridging the gap between the kinetic- and the hydrodynamic transport regimes.

Keywords: negative ion mobility, supercritical Ne gas, free volume model.

Submitted to: *Plasma Sources Sci. Technol.*

The knowledge of how ions drift through a gas or liquid under the action of an electric field is very important for both applications and fundamental science in physics and chemistry. The theory of ion transport is basic for many applications of low temperature plasmas [1–3] in biology, chemical synthesis, electrical discharges, high-energy physics [4], and is also fundamental to shed light on the kinetic processes related to the complex interaction between charges and environment. In low-density gases the Kinetic Theory describes the ion mobility μ via the momentum transfer scattering cross section determined by the ion-atom interaction potential [5]. In high-density environments, the motion of thermal ions occurs in the hydrodynamic regime and the Stokes formula can be used to describe μ by introducing an effective hydrodynamic radius R. In this case the ions are used to probe the microscopic structure and behavior of liquids such as superfluid He (for a review, see [6]), hydrocarbons [7,8], and cryogenic liquids [9–11]. However, a unified theory (or model) describing how the ion transport behavior crosses over from the kinetic- to the hydrodynamic regime is still missing. Supercritical gases, whose density can be varied in an extremely broad range, offer a unique test field to seek for a solution that bridges the gap between dilute gas and liquid.

Whereas the behavior of cations is amply investigated because are easily produced by direct ionization of the sample by means of high-energy radiation or electrical discharges, negative ions are not as thoroughly studied in spite of their relevance, e.g., in the physical chemistry of the atmosphere [12], because are produced by the quite inefficient, resonant, low-energy electron attachment process to electronegative molecular impurities [13]. A temporary anion formed in a vibrationally excited state [14, 15] rapidly decays by autodetachment unless it is stabilised by collisions with host gas atoms [16–20]. The processes leading to the formation of stable anions depend on the environment and give origin to states which cannot be adiabatically result by the addition of the ion to the environment [21] and whose structure is more complicated than that of cations [22]. Among electronegative impurities such as CO_2 [23], NO [24], and SF_6 [25], O_2 [26], whose electron affinity is $\approx 0.45\,\mathrm{eV}$ [27], plays the most important role because its ubiquitous presence as impurity even in the best purified gas makes the same ionic species, O_2^-, available to probe sample specific features. The mobility of O_2^- has been investigated only in few experiments: in liquid Ar and Kr [9] and Xe [9, 11, 28] and in supercritical He [29, 30], Ne [30, 31], and Ar [32, 33]. Here, we report new results obtained in Neon gas on several isotherms in a broad density range and show how the experimental results are very well rationalized by a recent thermodynamical model aimed at predicting the ion hydrodynamic radius [34–38].

The experiment is based on the pulsed Townsend electron photoinjection technique. The technical details of the experiments are described in literature [31]. Ions are produced by resonant electron attachment to O_2 impurities in a concentration of a few tens of ppm. The drift field is so weak that the density normalized field E/N never exceeds a few tens of mTd ($1\,\mathrm{Td} = 10^{-21}\,\mathrm{V\,m^2}$). Thus, the ions always are in thermal equilibrium with the gas and μ does not depend on E/N, as shown in Fig. (1).

The theoretical interpretation of such measurements is still unsatisfactory. In the

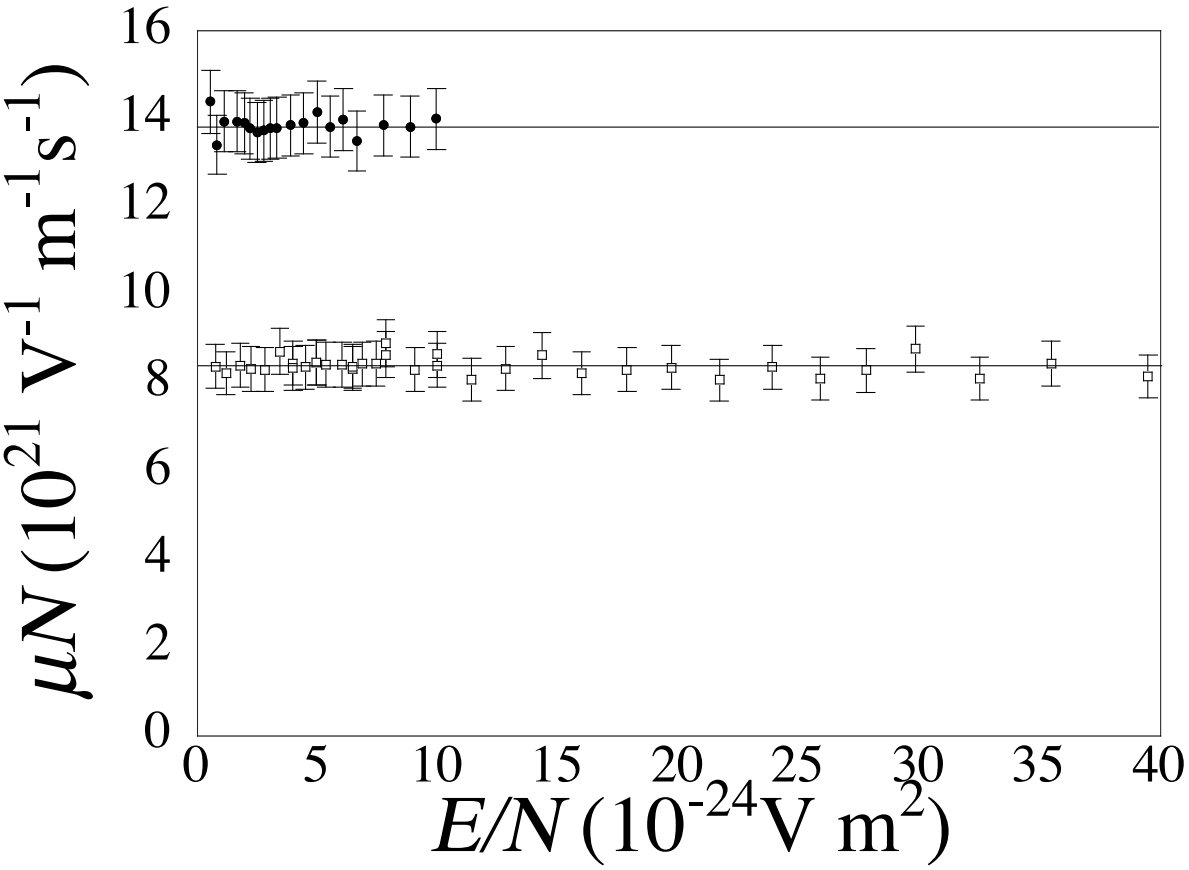

Figure 1. μN vs E/N of O_2^- in Ne gas at $T = 45\,\mathrm{K}$. Closed points: $N = 23.45\,\mathrm{nm}^{-3}$. Open points: $N = 2.63\,\mathrm{nm}^{-3}$.

gas at low- up to intermediate N along isotherms the experimental density normalized mobility μN showed a small, though unmistakable, almost linear dependence on N [30]. This dependence is also present in the new measurements displayed in Fig. (2) whereas, according to the Kinetic Theory [39], μN should be constant

$$\mu N = \frac{3e}{8\pi R^2}\left(\frac{\pi}{2m_r k_\mathrm{B} T}\right)^{1/2} \tag{1}$$

in which R is the hard-sphere radius of the ion and m_r is the ion-atom reduced mass. Moreover, the low density limit of μN disagrees by a factor ≈ 2 with the Langevin's prediction [5, 31, 40].

By contrast, at densities comparable to those of a liquid, the ion mobility cannot simply be described by the hydrodynamic Stokes formula with a constant hydrodynamic radius R

$$\mu = \frac{e}{6\pi\eta R} \tag{2}$$

in which η is the viscosity, even if the Navier-Stokes (NS) equations are solved by taking into account the density and viscosity non-uniformities induced by electrostriction [31, 41] (dashed line in Fig. (3), in which the experimental data for $T = 45\,\mathrm{K}$ [31] are shown).

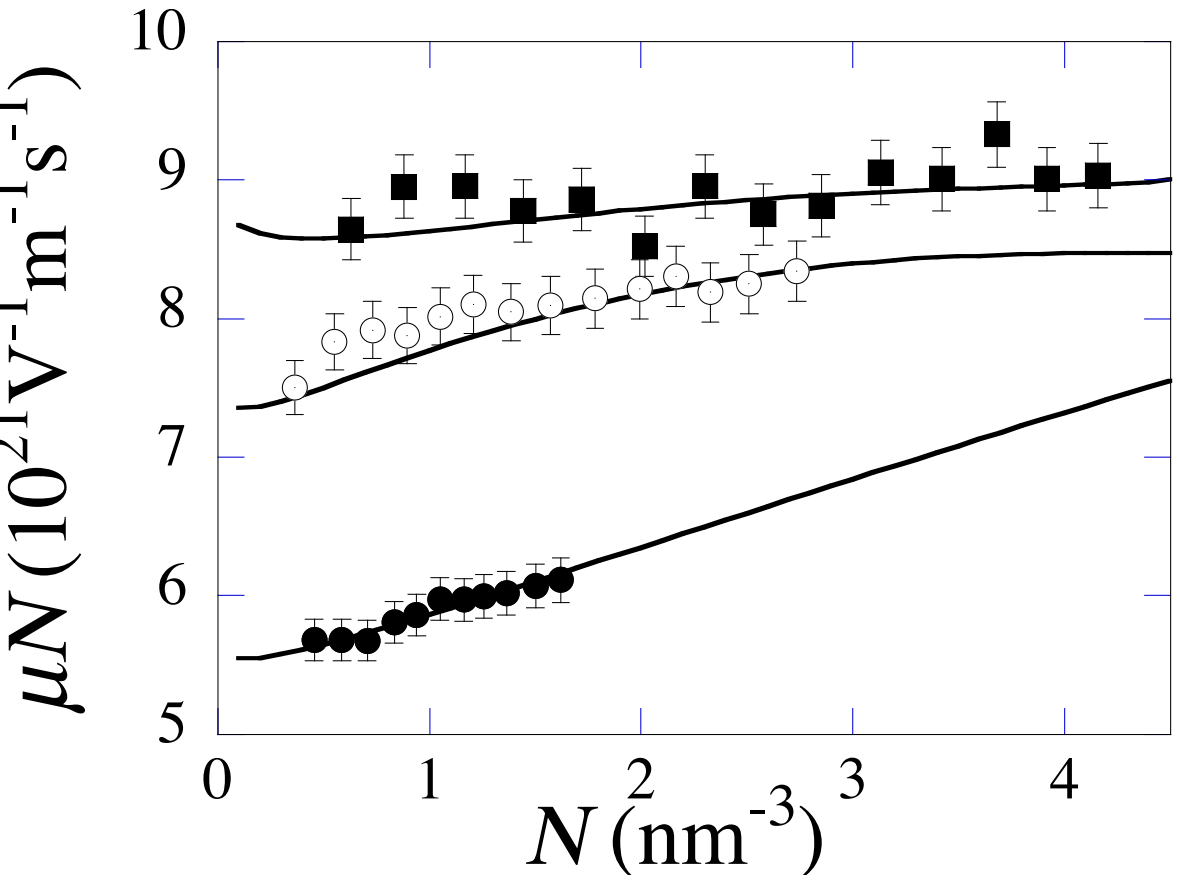

Figure 2. μN vs N for some isotherms. From top: $T = 130.8\,, 64.4\,,$ and $334\,\mathrm{K}$. Lines: model prediction.

A great improvement of the rationalization of the experiments has been achieved by accounting for the structure of the O_2^- ion [42,43]. Besides the solvation shell formed by electrostriction [44], the additional electron interacts with the electronic shells of the surrounding atoms via repulsive exchange forces that overwhelm the attractive polarization interaction and a void is created around the bare ion. So, the transport is determined by the interaction of such large complex structure with the gas and is quite insensitive to the ionic species. Detailed calculations [42, 43] yield the void radius R by minimizing the free energy of the complex and obtain the gas density profile established around the ion. R turns out to be almost independent of N whereas the local density profile induced by electrostriction strongly depends on the polarizability of the gas. In Ne the measurements were carried out $T \approx 45\,\mathrm{K}$ [31], i.e., very close to the critical temperature when the gas is most compressible. As a consequence of its large polarizability, size and density of the solvation shell cannot be neglected. At the largest N the mean free path and the mean interatomic separation are much smaller than the cavity size and the hydrodynamic Stokes formula Eq. (2) is used to describe μ. The position of the maximum of the density profile is chosen as hydrodynamic radius and η is evaluated at the density of the maximum. The agreement with the data is quite

reasonable for $15\,\mathrm{nm}^{-3} \leq N \leq 25\,\mathrm{nm}^{-3}$ but it fails at reproducing the data for smaller N and the crossover between Knudsen- and hydrodynamic regime [42] (dotted line in Fig. (3)).

Recently, a heuristic model has appeared which successfully rationalizes electron and cation mobility in liquid and supercritical He [34–38]. The model is based on the free volume concept adopted in the past to predict properties such as the ionic conductivity in polymers [45] and the viscosity of liquids [46]. The model provides a thermodynamic equation of state (EOS) for the N and T dependence of the free volume V_f available for the ion motion. The linear size of the free volume per particle is assumed to be related to the effective radius in the Stokes formula. Electrons in liquid helium are fully solvated and are surrounded by a hollow cavity so that the volume per solvated particle is $V_s \propto V_f/N$, where $V_f = V - b$. V is the macroscopic volume occupied by the medium and b is the total solvent covolume. The covolume b' of ions is neglected because of their extremely low concentration. The thermodynamic description of V_s is

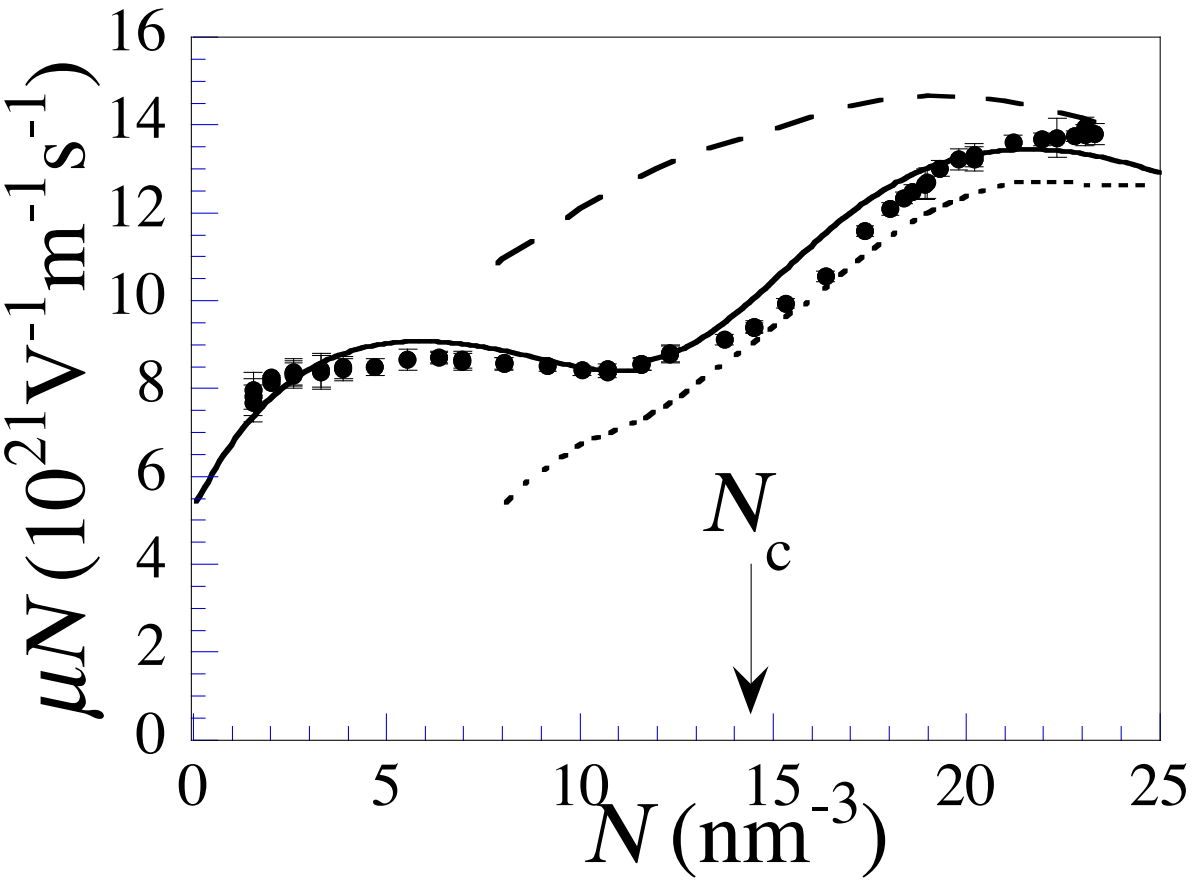

Figure 3. μN vs N for O_2^- ions in Ne gas at $T = 45\,\mathrm{K}$ [31]. Dashed line: solution of the NS equation accounting for the electrostriction induced nonuniformities. Dotted line: Khrapak's model [42]. Solid line: present model.

accomplished by a van der Waals-like EOS

$$V_s = \frac{k_{\mathrm{B}}T}{P+\Pi} \tag{3}$$

in which P is the ordinary pressure and Π is the internal pressure that accounts for the attractive potential energy contributions in the system. For a fully developed solvation shell of spherical shape, its linear size is simply given by $R - R_0 = (3V_s/4\pi)^{1/3}$, where R_0 is the hard-sphere radius of the charge-medium interaction. By contrast, for ions in a supercritical gas, compressibility effects have to be taken into account. At constant T , the solvation shell size follows the behavior of the compressibility [47, 48]. Starting from low N the shell is gradually growing up along with the compressibility. At higher N compressibility and size reach a maximum and then decrease with a further density increase whereas the free volume is a monotonic function of N. Thus, we expect that both V_s and $R - R_0 = g(V_f/N)$ are functions of V_f/N. The analytical forms of Π and g have to be determined by enforcing agreement with the experimental results.

At high N, where the Knudsen number, , i.e., the ratio of the atom mean free path ℓ to the size of the ion R, is $K_n = \ell/R \ll 1$, the ion drift occurs in the hydrodynamic regime described by the Stokes formula. However, as most of the experimental data fall in the transition region from the hydrodynamic- to the kinetic regime in which $K_n \gg 1$, we extend the predictive range of the model by using the empirical Millikan-Cunningham interpolation formula for the mobility [49–51]

$$\mu N = \frac{eN}{6\pi\eta R}\left\{1 + \phi\left[K_n(T,N)\right]\right\} \tag{4}$$

This approach has quite successfully been pursued, for instance, for localized electrons in dense He [52] and Ne gas [53]. The slip correction factor ϕ must vanish at high N and, for large K_n at low N, it must be such that μ is given by Eq. (1). Several analytic forms are proposed in literature (for a review, see [54]), but we have chosen the present one by enforcing agreement with the data.

The published Neon data at $T = 45\,\mathrm{K}$ [31] span a broad density range $0.17 \lesssim N/N_c \lesssim 1.7$ that almost entirely covers the crossover region and their re-analysis allows us to fix all the model parameters. According to the Occam's razor principle [55] we have tried to keep their number as small as possible. Firstly, the simplest choice for the internal pressure term far away from any phase transition is

$$\Pi(N,T) = \alpha N^2 \tag{5}$$

The α parameter determines the density of the compressibility maximum. The experimental data show a shallow minimum around $N_m \approx 11.5\,\mathrm{nm}^{-3}$. Thus, it is reasonable to assume that the effective ion radius is maximum for this density value where the system compressibility is the largest. This observation yields $\alpha = 8.937 \times 10^5\,\mathrm{Pa\,nm}^6$. It is extremely interesting to note that the same value gives good agreement with the data in liquid and supercritical He [34–38]. α, which is related to the attractive interactions, appears to be system independent, being thus endowed with some sort of universal character.

We expect that the effective ion radius at constant T is given by a functional form of the scaled free volume V_0/V_s, in which V_0 belongs to a suitable reference state, identical to that which allowed the rationalization of other mobility measurements [34–38]

$$\frac{R}{R_0} = 1 + \frac{(V_0/V_s)^{\epsilon_1}}{1 + \gamma\,(V_0/V_s)^{\epsilon_1} \exp\left[-K(T)\,(V_0/V_s)^{\epsilon_2}\right]} \tag{6}$$

By casting Eq. (3) in the form

$$\frac{V_0}{V_s} = \delta \frac{P + \Pi}{T} \tag{7}$$

with $\delta = 0.15$, a fit of the mobility data at the highest N gives the values $R_0 \approx 0.315\,\mathrm{nm}$, $\epsilon_1 = 1/2$, $\epsilon_2 = -1$, and $\gamma = 6.3$. For the Neon EOS we used literature data [56]. We emphasize that the analytical form of Eq. (6) has been determined by investigating several possibilities and picking the simplest form provided that it minimizes the deviations from the data. We also note that this analytical form is valid for all other mobility measurements [34–38].

An analysis of the data for $T > 45\,\mathrm{K}$ shows that $K(T)$ roughly describes an exponentially decreasing function of T/T_c. Its best form is

$$K(T) = k_1 \mathrm{e}^{-\zeta T/T_c} + k_2 \mathrm{e}^{-(|T/T_c - \xi|/2)^3} \tag{8}$$

with $k_1 = 148.05$, $k_2 = 2.0285$, $\zeta = 2.0279$, and $\xi = 3$. Its physical meaning is that it makes the effective radius more sensitive to the free volume at low T whereas it guarantees that, at higher T and low N, the effective radius roughly tends to the hard-sphere radius of the ion-atom interaction potential.

For the slip factor correction we used a modified version of the formula proposed by Knudsen *et al.* [57, 58] in order to account for objects whose size may depend on T and N

$$\phi(N,T) = \frac{1}{2}\frac{N_c}{N} \mathrm{e}^{-[\chi(T)/K_n(N,T)]^{3/4}} \mathrm{e}^{T_c/T} \left(1 - \mathrm{e}^{-T/T_c}\right) \tag{9}$$

In order to evaluate the Knudsen number we used the experimental determination of the mean free path from the viscosity as prescribed by the Kinetic Theory [59]

$$\ell = \frac{3\eta(N,T)}{N m_r \bar{v}} \tag{10}$$

in which $\bar{v} = [8k_\mathrm{B}T/\pi m_r]^{1/2}$ is the mean thermal velocity. η is computed with NIST software.

The analysis of the data at higher T requires the introduction of a temperature dependence in the slip factor by the function $\chi(T)$ which is approximately constant in the $65\,\mathrm{K} < T < 250\,\mathrm{K}$ range but slightly increases the correction factor at higher T and reduces it at lower T. Its role can heuristically be understood by noting that it favors the ion hydrodynamic drift behavior at lower T where the formation of a solvation shell is easier. Its best form is

$$\chi(T) = \chi_1 \mathrm{e}^{-\zeta_2 T/T_c} + \chi_2 \mathrm{e}^{-(|T/T_c - \xi_2|/\zeta_2)^{\chi_3}} \tag{11}$$

with $\chi_1 = 36.479$, $\zeta_2 = 2.6931$, $\chi_2 = 0.957$, $\xi_2 = 3.2117$, and $\chi_3 = 7.8475$. At the same time the factor $e^{T_c/T}(1 - e^{-T/T_c})$ has been included in order to obtain agreement with the temperature dependent, low-density limit of the experimental data.

We have to note, however, that at all densities of all isotherms, even at the largest density attained on the coldest isotherm, the Knudsen number is sufficiently large as to actually make the exponential in the slip factor in Eq. (9) density independent. As a result, the slip factor is mainly inversely proportional to N and can be extremely well approximated by the functional form $\phi(N, T) = A(T)/N$ where A only depends on T.

The model prediction for $T = 45\,\mathrm{K}$ is the solid line in Fig. (3). It is interesting to note that the agreement with the data, though still not perfect, is now obtained over the entire density range thereby bridging the kinetic- and hydrodynamic transport regimes.

It also interesting to compare in Fig. (4) the hydrodynamic radius given by Eq. (6) and the effective hydrodynamic radius

$$R_{\mathrm{eff}} = \frac{R}{1 + \phi(N, T)} \tag{12}$$

with its experimental determination obtained by inverting the Stokes formula. First of all, we note that the experimental radius shows a maximum at precisely the same density of the shallow minimum in μN. The hydrodynamic radius computed by Eq. (6)

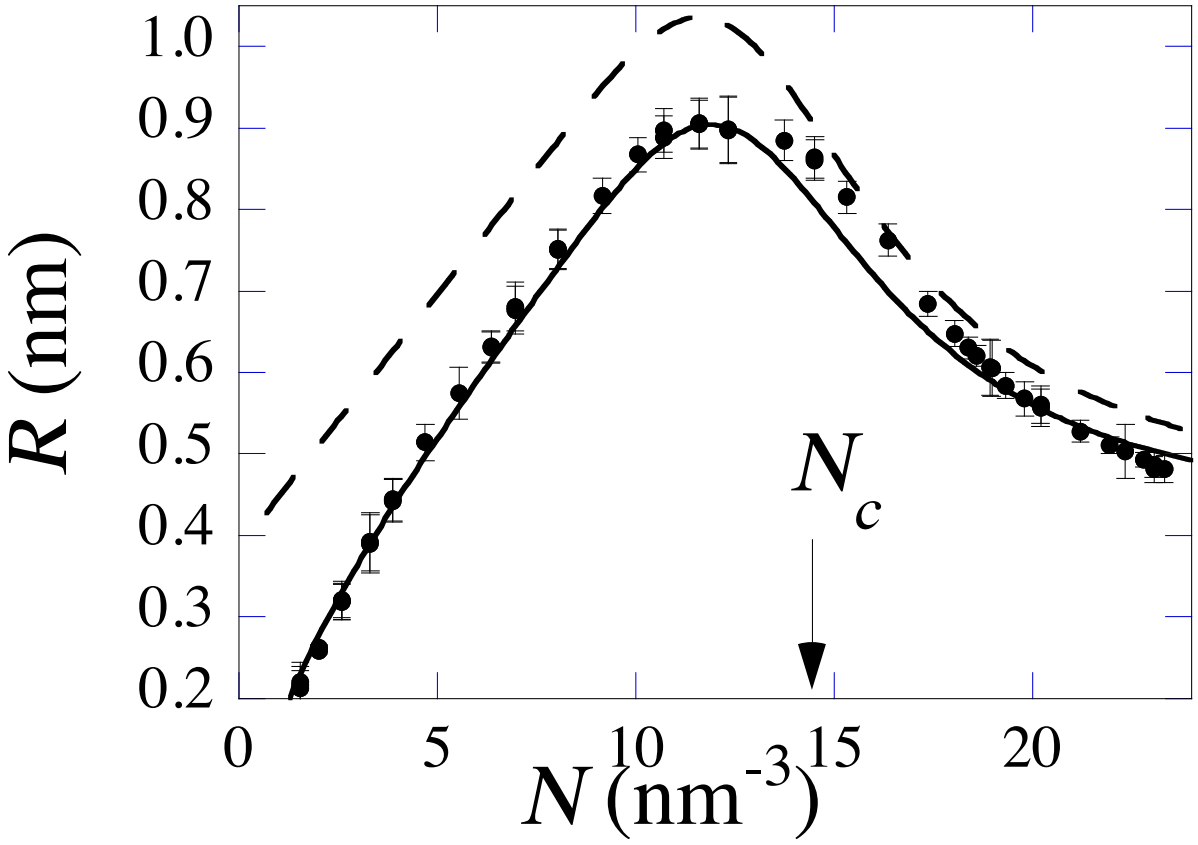

Figure 4. R vs N for $T = 45\,\mathrm{K}$. Dashed line: Eq. (6). Solid line: Eq. (12). Points: experimental determination.

shares the same behavior although it is more than 20 % larger. However, if the slip factor is accounted for, the experimental and the computed radii are in very good agreement.

The position of the maximum is fixed by the choice of the α parameter that contains all the contributions of the attractive potential energy in the system. The compressibility is maximum when the attraction and repulsion forces between atoms are in balance so that the atoms can more easily rearrange themselves to build local structures without too large a free energy cost [48]. Actually, the maximum compressibility of the pure gas occurs for N_c, whereas the presence of the strong attractive ion-atom polarization interaction increases the gas compressibility by shifting its maximum to a lower N.

As no theory for the α parameter is available, we believe that its apparent universality feature might be related to the Law of Corresponding States stemming from the use of a van der Waals-like EOS. The α parameter describes how the compressibility of a system is perturbed by the injection of excess charges. The Π term of the pure fluid is already accounted for in its $P(N,T)$ EOS. Hence, the present Π contribution is actually the difference between the attractive interactions in the system with and without the excess charges and should therefore be fluid independent, as long as the charge concentration is small enough.

Although all parameters in the free volume model have mainly been determined by seeking for agreement with the low T data, we have applied the model to all 15 investigated isotherms by keeping the parameters fixed at the values determined at low T. In Fig. (2) we compare the model prediction with the experimental data on three higher isotherms. We see that the model is remarkably successful at describing the N and T dependence of the experimental data.

In conclusion, we have measured the mobility of Oxygen ions in supercritical Neon gas for $45\,\mathrm{K} < T < 334\,\mathrm{K}$ and adopted the free volume model to compute the hydrodynamic radius of the complex that is formed as a balance between long range attractive polarization interaction and short range repulsive exchange forces when an ion is embedded in a fluid. The variation of the hydrodynamic radius that at first increases with N, reaches a maximum for $N_m < N_c$, and then decreases as N is increased further can be interpreted as the condensation, growth and compression of negatively charged clusters [37]. Remarkably, in the present case the clusters are formed around a cavity surrounded by a solvation shell in which a negative ion is embedded. Thus, the measurements of the O_2^- mobility in a non polar solvent yield pieces of information specific to the solvation shell because the ion core can safely be expected to stay unchanged owing to the strong short-range repulsive exchange forces and any change of the cluster size has to be attributed to changes of the thickness of the solvation shell itself.

In order that the description of the mobility bridges the low-density kinetic transport regime and the high-density hydrodynamic one we used a modified version of the Millikan-Cunningham slip factor. We have to stress the fact that a good description of the density dependence of the mobility data on all isotherms is obtained by using the parameter values that are mainly determined from the analysis of the low temperature

data. In spite of the fact that some experimental observations cannot fully be explained by the present approach, such as a residual, extremely weak field dependence of μ at low N and high T, we are confident that these results are promising to extend the investigation to negative ions in other noble gases as well as to positive ions in different fluids.

Acknowledgments

The authors wish to thank K. von Haeften for critical reading of the manuscript.

References

[1] Bruggeman P J et al. 2016 *Plasma Sources Sci. Technol.* **25** 053002
[2] Adamovich I et al. 2017 *J. Phys. D. Appl. Phys.* **50** 323001
[3] Schmidt W F and Yoshino K 2005 *Electronic Excitations in Liquefied Rare Gases* (Stevenson Ranch, CA (USA): American Scientific Publishers) chap Electric Discharges, pp 296–315
[4] Lopez I M and Chepel V 2005 *Electronic Excitations in Liquefied Rare Gases* (Stevenson Ranch, CA (USA): American Scientific Publishers) chap Rare Gas Liquid Detectors, pp 331–388
[5] Mason E A and McDaniel E W 1988 *Transport Properties of Ions in Gases* (New York: Wiley)
[6] Borghesani A F 2007 *Ions and Electrons in Liquid Helium* (International Series of Monographs on Physics vol 137) (Oxford: Oxford University Press)
[7] Gee N and Freeman G R 1980 *Can. J. Chem.* **58** 1490–1494
[8] Huang S S and Freeman G R 1980 *J. Chem. Phys.* **72** 1989–1993
[9] Davis H T, Rice S A and Meyer L 1962 *J. Chem. Phys.* **37** 2470–2472
[10] Gee N, Floriano M A, Wada T, Huang S S S and Freeman G R 1985 *J. Appl. Phys.* **57** 1097–1101
[11] Schmidt W F, Hilt O, Illenberger E and Khrapak A G 2005 *Radiat. Phys. Chem.* **74** 152–159
[12] Hughes P and Mason N 2001 *Introduction to Environmental Physics: Planet Earth, Life and Climate* (Boca Raton: CRC Press)
[13] Christophorou L G, McCorkle D L and Christodoulides A A 1984 *Electron-Molecule Interactions and Their Applications* vol I (Orlando: Academic Press) chap Electron Attachment Processes
[14] Illenberger E 1994 *Linking the Gaseous and Condesed Phases of Matter, The Behavior of Slow Electrons* (*NATO ASI Series B: Physics* vol 326) (New York: Plenum Press) chap Electron Attachment to Molecules, pp 355–376
[15] Matejcik S, Kiendler A, Stampfli P, Stamatovic A and Mářk T D 1996 *Phys. Rev. Lett.* **77** 3771–3774
[16] Bloch F and Bradbury N E 1935 *Phys. Rev.* **48** 689–695
[17] Bartels A 1973 *Phys. Lett. A* **45** 491–492
[18] Bruschi L, Santini M and Torzo G 1984 *J. Phys. B At. Mol. Phys.* **17** 1137–1154
[19] Borghesani A F and Santini M 1991 Electron Localization Effects and Resonant Attachment to O_2 Impurities in Highly Compressed Neon Gas *Gaseous Dielectrics VI* ed Christophorou L G and Sauers I (New York: Plenum Press) pp 27–33
[20] Neri D, Borghesani A F and Santini M 1997 *Phys. Rev. E* **56** 2137–2142
[21] Hernandez J P 1991 *Rev. Mod. Phys.* **63** 675–697
[22] Khrapak A G, Tegeder P, Illenberger E and Schmidt W F 1999 *Chem. Phys. Lett.* **310** 557–560
[23] Nishikawa M, Itoh K and Holroyd R A 1999 *J. Phys. Chem. A* **103** 550–556
[24] Nishikawa M, Holroyd R and Itoh K 1998 *J. Phys. Chem. B* **102** 4189–4192
[25] Fehsenfeld F C 1970 *J. Chem. Phys.* **53** 2000–2004
[26] Bradbury N E 1933 *Phys. Rev.* **44** 883–890
[27] Travers A J, Cowles D C and Ellison G B 1989 *Chem. Phys. Lett.* **164** 449–455

[28] Hilt O, Schmidt W F and Khrapak A G 1994 *IEEE Trans. Dielectr. Electr. Insul.* **1** 648–656
[29] Bartels A 1975 *Appl. Phys.* **8** 59–64
[30] Borghesani A F, Chiminello F, Neri D and Santini M 1995 *Int. J. Thermophys.* **16** 1235–1244
[31] Borghesani A F, Neri D and Santini M 1993 *Phys. Rev. E* **48** 1379–1389
[32] Borghesani A F, Neri D and Barbarotto A 1997 *Chem. Phys. Lett.* **267** 116–122
[33] Borghesani A, Neri D and Barbarotto A 1999 *Int. J. Thermophys.* **20** 899–909
[34] Aitken F, Li Z L, Bonifaci N, Denat A and von Haeften K 2011 *Phys. Chem. Chem. Phys.* **13** 719–724
[35] Aitken F, Bonifaci N, Denat A and Von Haeften K 2011 *J. Low Temp. Phys.* **162** 702–709
[36] Aitken F, Bonifaci N, Mendoza-Luna L G and von Haeften K 2015 *Phys. Chem. Chem. Phys.* **17** 18535–18540
[37] Tarchouna H G, Bonifaci N, Aitken F, Mendoza Luna L G and von Haeften K 2015 *J. Phys. Chem. Lett.* **6** 3036–3040
[38] Aitken F, Volino F, Mendoza-Luna L, Haeften K and Eloranta J 2017 *Phys. Chem. Chem. Phys.* **19** 15821–15832
[39] Kihara T 1953 *Rev. Mod. Phys.* **25** 844–852
[40] Langevin M P 1905 *Ann. Chim. Phys.* 245–288
[41] Ostermeier R M and Schwarz K W 1972 *Phys. Rev. A* **5** 2510–2519
[42] Volykhin K F and Khrapak A G 1995 *JETP* **81** 901–908
[43] Khrapak A G, Schmidt W F and Volykhin K F 1995 *Phys. Rev. E* **51** 4804–4806
[44] Atkins K R 1959 *Phys. Rev.* **116** 1339–1343
[45] Miyamoto T and Shibayama K 1973 *J. Appl. Phys.* **44**
[46] Doolittle A K 1951 *J. Appl. Phys.* **22** 1471–1475
[47] Itoh K, Holroyd R a and Nishikawa M 2001 *J. Phys. Chem. A* **105** 703–709
[48] Itoh K, Muraoka K, Nagata T, Nishikawa M and Holroyd R 2004 *J. Phys. Chem. B* **108** 10177–10184
[49] Cunningham E 1910 **83** 357–365
[50] Millikan R A 1910 *Science* **32** 436–448
[51] Tyndall A M 1938 *The mobility of positive ions in gases* (Cambridge: The University Press)
[52] Levine J L and Sanders T M J 1967 *Phys. Rev.* **154** 138–149
[53] Borghesani A F and Santini M 1990 *Phys. Rev. A* **42** 7377–7388
[54] Allen M and Raabe O 1982 *J. Aerosol Sci.* **13** 537–547
[55] Priest G and Read S 1981 *Mind* **90** 274–279
[56] Katti R, Jacobsen R, Stewart R and Jahangiri M 1986 *Adv. Cryo. Eng.* **31** 1189–1197
[57] Knudsen M and Weber S 1911 *Ann. Phys.* **341** 981–994
[58] Kim J, Mulholland G, Kukuck S and Pui D 2005 *J. Res. Natl. Inst. Stand. Technol.* **110** 31–54
[59] Reif F 1985 *Fundamentals of Statistical and Thermal Physics* (Auckland: McGraw-Hill)